

## ORIGINAL ARTICLE

**Molecular mimicry in inducing DNA damage between HIV-1 Vpr and the anticancer agent, cisplatin**K Siddiqui<sup>1</sup>, L Del Valle<sup>2</sup>, N Morellet<sup>3</sup>, J Cui<sup>2</sup>, M Ghafouri<sup>2</sup>, R Mukerjee<sup>2</sup>, K Urbanska<sup>2,4</sup>, S Fan<sup>2</sup>, CB Pattillo<sup>5</sup>, SL Deshmane<sup>2</sup>, MF Kiani<sup>5</sup>, R Ansari<sup>5</sup>, K Khalili<sup>2</sup>, BP Roques<sup>3</sup>, K Reiss<sup>2</sup>, S Bouaziz<sup>3</sup>, S Amini<sup>1</sup>, A Srinivasan<sup>6</sup> and BE Sawaya<sup>2</sup>

<sup>1</sup>Department of Biology, College of Science and Technology, Temple University, Philadelphia, PA, USA; <sup>2</sup>Department of Neuroscience and Center for Neurovirology, Temple University School of Medicine, Temple University, Philadelphia, PA, USA; <sup>3</sup>Unite de Pharmacologie Chimique et Genetique, INSERM, Avenue de l'Observatoire, Paris Cedex 06, France; <sup>4</sup>Department of Cell Biology, Faculty of Biotechnology, Jagiellonian University, Krakow, Poland; <sup>5</sup>Department of Mechanical Engineering, Temple University, Philadelphia, PA, USA and <sup>6</sup>Department of Microbiology and Immunology, Kimmel Cancer Center, Thomas Jefferson University, Philadelphia, PA, USA

**The human immunodeficiency virus type 1 (HIV-1) viral protein R (*vpr*) gene is an evolutionarily conserved gene among the primate lentiviruses. Several functions are attributed to Vpr including the ability to cause cell death, cell cycle arrest, apoptosis and DNA damage. The Vpr domain responsible for DNA damage as well as the mechanism(s) through which Vpr induces this damage is unknown. Using site-directed mutagenesis, we identified the helical domain II within Vpr (aa 37–50) as the region responsible for causing DNA damage. Interestingly, Vpr  $\Delta$ (37–50) failed to cause cell cycle arrest or apoptosis, to induce Ku70 or Ku80 and to suppress tumor growth, but maintained its capability to activate the HIV-1 LTR, to localize to the nucleus and to promote nonhomologous end-joining. In addition, our cytogenetic data indicated that helical domain II induced chromosomal aberrations, which mimicked those induced by cisplatin, an anticancer agent. This novel molecular mimicry function of Vpr might lead to its potential therapeutic use as a tumor suppressor.**

*Oncogene* (2008) 27, 32–43; doi:10.1038/sj.onc.1210632; published online 23 July 2007

**Keywords:** HIV-1; Vpr; DNA damage; chromosomal aberrations; cisplatin; necrosis

**Introduction**

The 14 kDa human immunodeficiency virus type 1 (HIV-1) accessory protein, viral protein R (Vpr), has received significant attention due to its regulatory effect

upon virus and host functions (le Rouzic and Benichou, 2005). At the cellular level, expression of Vpr results in deregulation of the cell cycle and accumulation of cells at the G<sub>2</sub>/M stage of the cell cycle, which leads to their death by apoptosis (Goh *et al.*, 1998; Sawaya *et al.*, 1999; Tachiwana *et al.*, 2006). Vpr can induce apoptosis through a variety of mechanisms (Jacotot *et al.*, 2000; Patel *et al.*, 2000; Stewart *et al.*, 2000). In one study, suppression of nuclear factor- $\kappa$ B (NF- $\kappa$ B) activity through the induction of I $\kappa$ B was linked to Vpr-mediated apoptosis (Ayyavoo *et al.*, 1997). In other studies, induction of apoptosis by Vpr was attributed to rapid dissipation of the mitochondrial transmembrane potential, association of Vpr with the adenine nucleotide translocator, release of cytochrome *c* and activation of caspase-3 (Jacotot *et al.*, 2000). Finally, Vpr-induced apoptosis has been shown to require the activation of caspase-8 (Patel *et al.*, 2000), and be part of a pathway involving hHR23A (Gaynor and Chen, 2001). Vpr was also shown to induce cell death in rat astrocytes primarily by a necrotic mechanism (Huang *et al.*, 2000). Vpr exerts a transcriptional activation function in cells infected with HIV-1 similar to VP16 of Herpes simplex virus (Sherman *et al.*, 2002). Vpr can induce several promoters, including the HIV-1 LTR and p21<sup>WAF1</sup> (Wang *et al.*, 1995; Amini *et al.*, 2004). These studies suggest that cooperativity between several cellular proteins including Sp1 (Wang *et al.*, 1995), p300 (Kino *et al.*, 2002) and p53 (Sawaya *et al.*, 1998) is necessary for Vpr-induced regulation of the HIV-LTR. Vpr was also shown to cause cell differentiation and DNA damage (Shimura *et al.*, 1999a, b). In those reports, the authors demonstrated that Vpr induced chromosomal aberrations and gene amplification, but the domain(s) and mechanism(s) by which Vpr induced these anomalies were not identified. In a recent study, the same group demonstrated that Vpr induces double-strand breaks (DSBs) in HIV-1-infected cells (Tachiwana *et al.*, 2006). However, the Vpr domain responsible for this damage or DNA break was not identified.

Correspondence: Dr BE Sawaya, Department of Neuroscience and Center for Neurovirology, Temple University School of Medicine, Temple University, 1900 North 12th Street, Philadelphia, PA 19122, USA.

E-mail: sawaya@temple.edu

Received 28 November 2006; revised 17 May 2007; accepted 29 May 2007; published online 23 July 2007

Here, we identify the region spanning aa 37–50 within the full-length Vpr as a causative factor in the induction of a number of insults to the genome. The DNA of telomeric region is most likely involved in the DNA double-strand damage and rejoining, chromosomal numerical and structural aberrations, cell cycle arrest and apoptosis in cultured U87-MG cells. Furthermore, the 37–50 domain of wild-type (wt) Vpr induced chromosomal anomalies and exhibited molecular mimicking to cisplatin, an anticancer alkylating drug.

## Results

Several studies implicate Vpr in DNA damage; however, the precise domain within Vpr involved in this damage has not yet been elucidated (Tachiwana *et al.*, 2006). Using cytogenetic analysis, we examined the DNA-damaging effect of a specific domain of Vpr. U-87MG cells were transfected with Vpr expression plasmid, treated with colcemid, lysed in hypotonic buffer and fixed (Siddiqui *et al.*, 1988). As a positive control, cisplatin, an anticancer alkylating agent was used. As shown in Figure 1a, cisplatin as well as Vpr induced

DNA perturbation and structural chromosomal aberrations. The commonly noted aberrations are: quadriradial and formation of complex configurations of chromosomes (panels 1), ring, pulverized and dicentric chromosomes (panels 4). In addition, some metaphases exhibited chromosomes with amplified genes, for example, the presence of double minute chromosomes and stretched chromosomes (Vpr-0 panel). These abnormalities involve DNA breaks and end rejoining in a complex pattern. Some aberrations, especially the formation of complex configurations and dicentric chromosomes, are similar to aberrations induced by cisplatin (compare Vpr panels to cisplatin panels). No chromosomal anomalies were observed in the control cultures (Control panel). This suggests molecular mimicking between a biological entity (Vpr) and a chemical agent (cisplatin). The number of chromosomal aberrations and the type of aberrations are summarized in Figure 1b.

In the next set of experiments, we sought to identify the domain within Vpr responsible for DNA damage. Several Vpr mutants containing either point mutations or deletion of several amino acids were used (Wang *et al.*, 1995; Sawaya *et al.*, 1998, 1999; Zhou and Ratner, 2000). Vpr mutant expression plasmids were transfected

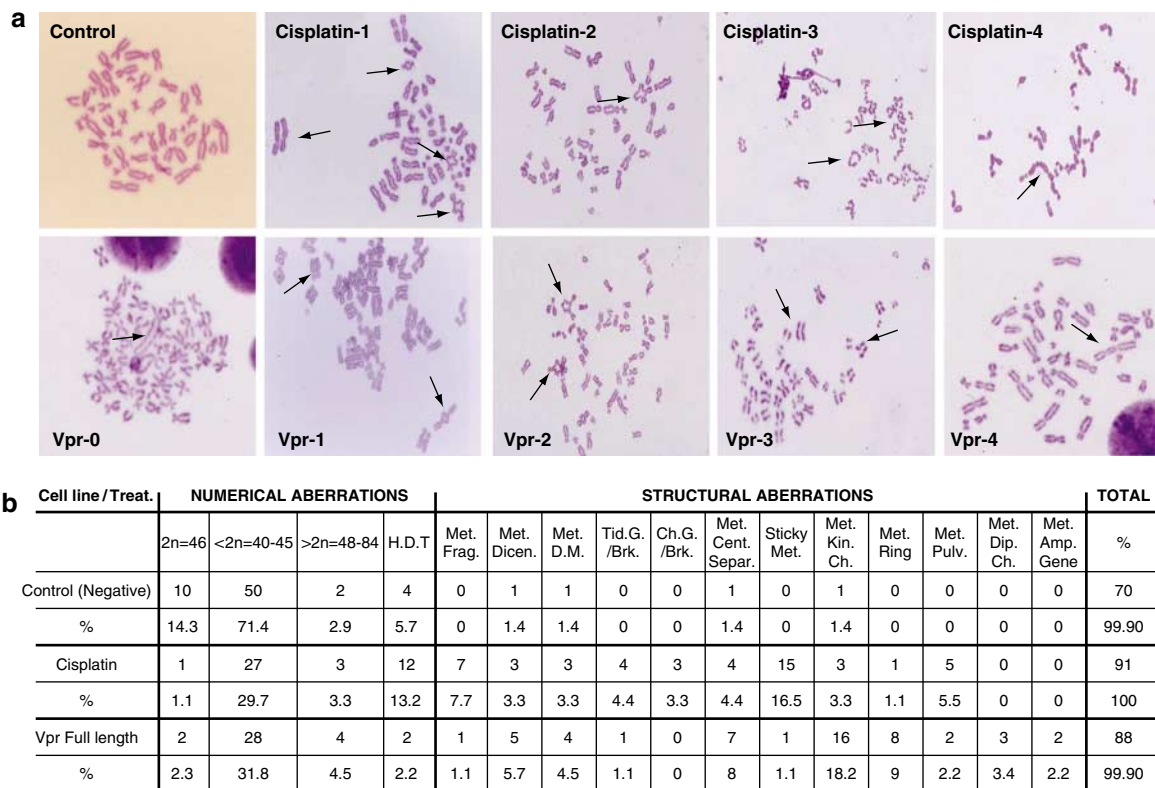


**Figure 1** Induction of chromosomal aberrations by Vpr and cisplatin. (a) Metaphase spreads were prepared from control and treated cultures. The arrows depict the aberrations. (b) The table presents the number and percentage of occurrence of numerical and structural chromosomal aberrations from control and treated cultures. H.D.T, hyperdiploid/tetraploid; Met. Frag., metaphase with fragment(s); Met. Dicen., metaphase with dicentric chromosome(s); Met. D.M., metaphase with double minute chromosome(s); Met. Cen. Sep., metaphase with separated centromers; Met. Kin. Ch., metaphase with kinky chromosomes; Met. Ring, metaphase with ring chromosomes; Met. Amp. Gene, metaphase with amplified gene chromosomes; Tid gap/brk, chromatid gap/break; Chr. gap/brk, chromosome gap/break; Stic. Met., sticky metaphase(s); Met. Pulv., pulverized metaphase; Met. Dip. Ch, diplochromosomes.

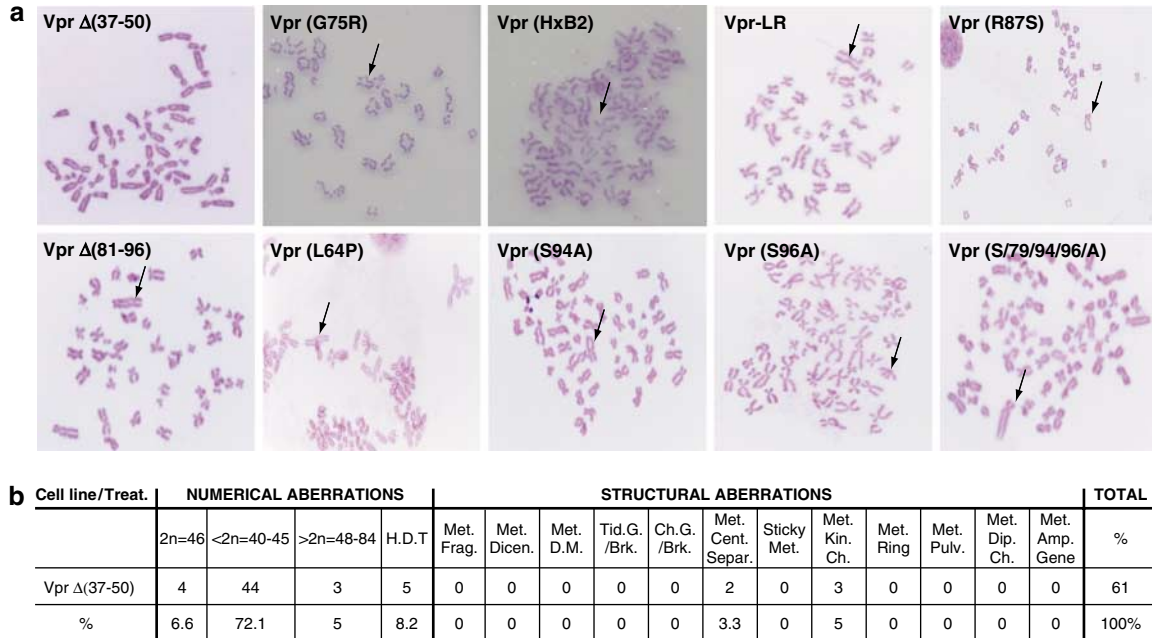


**Figure 2** Identification of the domain responsible for DNA damage. (a) Example of metaphases spread from cells treated with mutants Vpr as marked. Only Vpr  $\Delta(37-50)$  failed to cause chromosomal aberration. (b) Metaphase spreads were prepared from cells treated with Vpr mutant lacking residues (37–50) and the percentage of numerical and structural aberrations observed in these cells is presented. H.D.T, hyperdiploid/tetraploid; Met. Frag., metaphase with fragment(s); Met. Dicen., metaphase with dicentric chromosome(s); Met. D.M., metaphase with double minute chromosome(s); Met. Cent. Sep., metaphase with separated centromeres; Met. Kin. Ch., metaphase with kinky chromosomes; Met. Ring, metaphase with ring chromosomes; Met. Amp. Gene, metaphase with amplified gene chromosomes; Tid gap/brk, chromatid gap/break; Chr. gap/brk, chromosome gap/break; Stic. Met., sticky metaphase(s); Met. Pulv., pulverized metaphase; Met. Dip. Ch, diplochromosomes.

into U-87MG and subjected to cytogenetic analysis. As shown in Figure 2a, mutant Vpr induced DNA perturbation and structural chromosomal aberrations. These aberrations are similar to the ones observed with the full-length Vpr (compare Figure 2a to Figure 1a). Interestingly, only mutant Vpr  $\Delta(37-50)$ , in which amino acids 37–50 were deleted, did not produce chromosomal aberrations (Figures 2a and b). It should be noted that this region (aa 37–50) was previously shown to form the helical domain II of Vpr (Wecker *et al.*, 2002).

Previously, using MIT-23 cells, Tachiwana *et al.* (2006) demonstrated that the C-terminal domain of Vpr is involved in Vpr-induced DNA DSBs. Thus, we sought to examine the ability of this particular mutant to cause DNA damage. Using Vpr HxB2 in which 23 aa from the C-terminal domain were deleted (Mahalingam *et al.*, 1995), we observed that the most common anomalies caused by HxB2 were clumped metaphases, separated sister chromatids at kinetochore region, and metaphases with dumbbell-shaped chromosomes (Figure 2a, HxB2 panel). These anomalies indicate that no chromosomal break and rejoining occurred. These results led us to suggest that the C-terminal domain of Vpr is not involved in DNA damage and that the results obtained with this mutant in MIT-23 cells may be cell type-specific.

The inability of Vpr  $\Delta(37-50)$  to cause DNA damage led us to examine its stability and subcellular localization.

Using western blot analysis, U-87MG cells were transfected with Vpr (wt or mutant) expression plasmids. Figure 3a shows expression of transfected Vpr. Grb2 was the loading control. This experiment confirmed the expression and stability of Vpr  $\Delta(37-50)$  protein.

Next, U-87MG cells were infected with adeno-Vpr (full length or mutant). Uninfected or adeno-null infected cells were also used as controls. 4',6'-Diamidino-2-phenylindole hydrochloride (DAPI) staining was used to visualize nuclei (blue). As shown in Figure 3b, Vpr (red) is found in the nucleus and the cytoplasm. A similar localization was observed with Vpr  $\Delta(37-50)$ . Therefore, we concluded that both wt and mutant-Vpr proteins have a similar subcellular distribution.

The ability of wt Vpr to activate HIV-1 transcription led us to determine the functional ability of Vpr  $\Delta(37-50)$ . U-87MG cells were transfected with full-length LTR-CAT reporter gene construct, alone or in the presence of Vpr expression plasmid. As shown in Figure 3c, transfection of Vpr  $\Delta(37-50)$  activated HIV-LTR 5.12-fold, that is similar to wt Vpr.

Next, we examined whether Vpr  $\Delta(37-50)$  possesses the ability to cause cell cycle arrest at the G<sub>2</sub>/M checkpoint (Goh *et al.*, 1998). U-87 MG cells were transfected with enhanced green fluorescent protein (EGFP)-Spectrin plus Vpr or Vpr  $\Delta(37-50)$  expression plasmids, and later processed for fluorescence-activated cell sorting (FACS) analysis as described in Materials

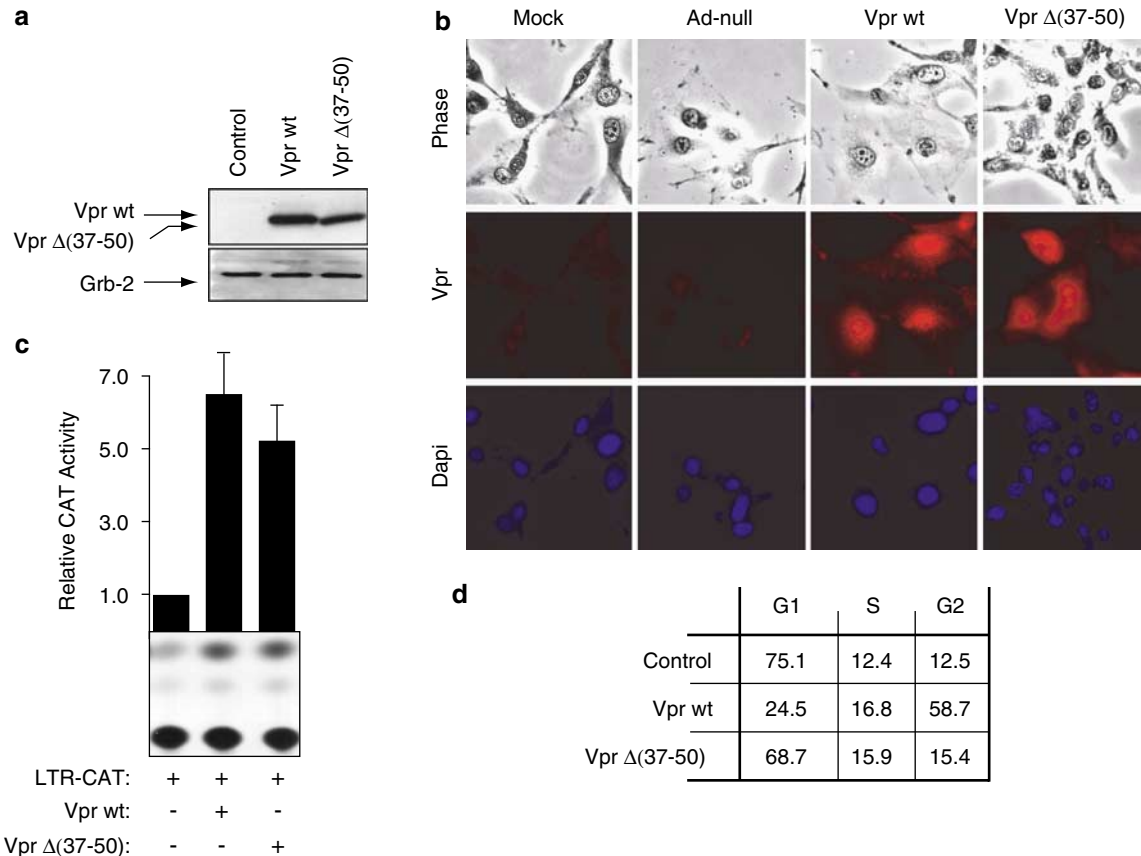


**Figure 3** Molecular functions of the (37–50) region. (a) U-87MG cells were transfected with 1.0  $\mu$ g of Vpr (full length or mutant) expression plasmids. Fifty microgram of total proteins was subjected to western blot analysis using anti-Vpr or -Grb2 antibodies, respectively. (b) U-87MG cells were mock-infected, adeno-null infected or infected with adenovirus-Vpr (full length or mutant) and analysed by immunocytochemistry assay. Anti-Vpr (red) antibody was tagged and used to detect the subcellular localization of Vpr. DAPI staining (blue) was used to identify the nuclear region. (c) U-87MG cells were transfected with LTR-CAT full length, either alone or in combination with plasmids expressing Vpr full length or mutant. CAT activities were determined after 48 h and presented as fold activation. The basal level of transcription was set at 1.0. The data represent the mean value of at least three separate transfection experiments. (d) U-87MG cells were synchronized by serum starvation. After 72 h, complete DMEM culture media containing 10% FCS was added. The cells were transfected with 10  $\mu$ g of plasmids expressing Vpr or Vpr  $\Delta$ (37–50) along with 2.5  $\mu$ g of a plasmid expressing EGFP-spectrin. After 36 h, cells were harvested, and processed for the measurement of their DNA content and EGFP expression by fluorescence-activated cell sorting. The percentage of cells in G<sub>1</sub>, S and G<sub>2</sub> is presented as a table.

and methods (Sawaya *et al.*, 2000). The cells transfected with expression vectors encoding wt Vpr exhibited cell cycle arrest in the G<sub>2</sub>/M (58.7%) of the cell cycle. However, the mutant Vpr was unable to induce cell cycle arrest in G<sub>2</sub>/M (Figure 3d). Thus, like wt Vpr, Vpr  $\Delta$ (37–50) is a stable protein, has the ability to activate HIV-LTR and is found in the nucleus and cytoplasm. However, it is unable to cause cell cycle arrest.

In preparation for cell division, nuclear chromatin undergoes critical rearrangement needed for the organization of chromosomes and their separation into daughter cells. These chromatin changes are initiated during G<sub>2</sub> phase of the cell cycle, and their most striking morphological manifestation is chromatin condensation (Hans and Dimitrov, 2001). Phosphorylation of histone H3 is highly correlated with the G<sub>2</sub> to M transition. In mitotic cells, H3 is specifically phosphorylated at serine 10 (S10) near its N terminus (Nowak and Corces, 2004). H3 dephosphorylation occurs rapidly after mitosis and S10 remains unphosphorylated throughout

the remainder of interphase (Juan *et al.*, 1998). Therefore, to further confirm that the Vpr-infected cells are in G<sub>2</sub> and not in mitotic phase, we performed western analysis. U-87MG cells were synchronized and then infected with adeno-null, adeno-Vpr or adeno-Vpr  $\Delta$ (37–50) viruses. Noninfected (mock) cells were used as a control. Cells were collected every 2 h, and nuclear extracts were prepared and subjected to western analysis using anti-cyclin B1 or antibody that recognizes H3 phosphorylated on S10. Note that this experiment was performed in duplicate where one set was subjected to cell cycle analysis (data not shown) and the other set was subjected to western blot analysis. As shown in Figure 4a, no changes were observed in the levels of cyclin B1 in Vpr-infected cells, which points to the accumulation of cyclin B1 in G<sub>2</sub> phase (left panels, adeno-Vpr row). Interestingly, S10-phosphorylated H3 was barely detectable in Vpr-infected cells (middle panels, Vpr row). These data confirm that the cells are in G<sub>2</sub> and almost no cells progressed to the M phase.

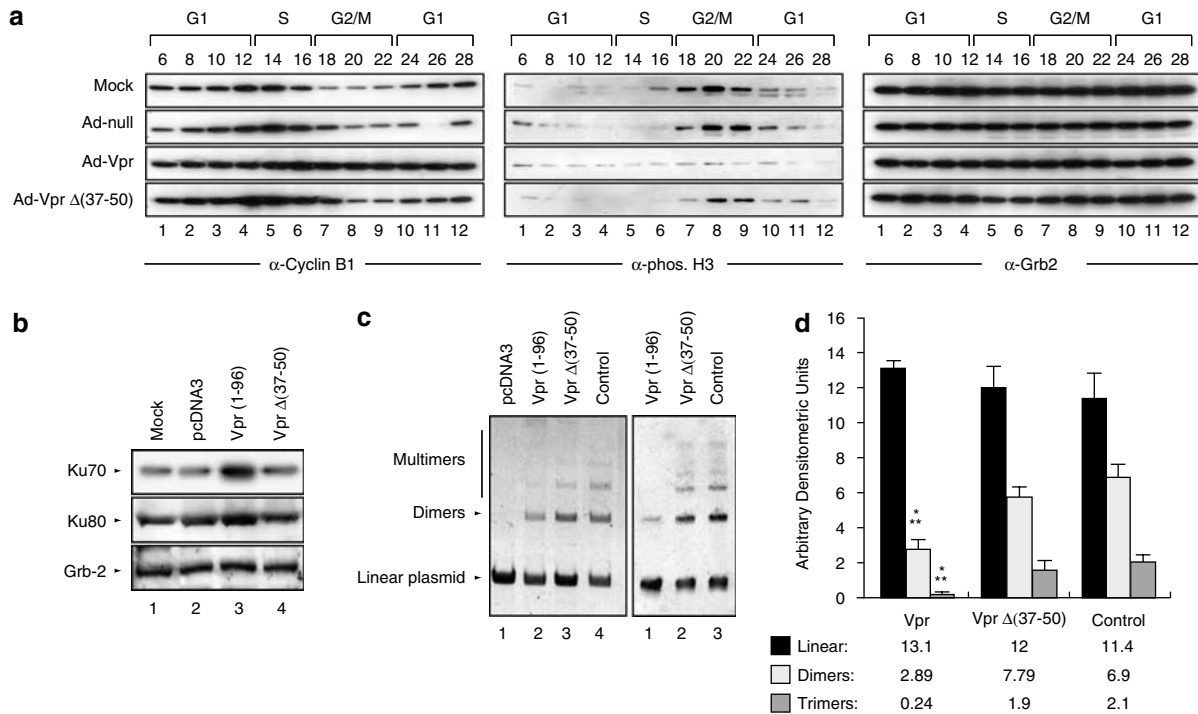


**Figure 4** Effect of Vpr and Vpr  $\Delta(37-50)$  on NHEJ. (a) U-87MG cells were synchronized and then infected with adeno-null, adeno-Vpr or adeno Vpr  $\Delta(37-50)$  viruses. Synchronized, uninfected (Mock) cells were used as a control. The cells were collected every 2 h as of the sixth hour after being released. Fifty micrograms of nuclear extracts were analysed by western blot with anti-cyclin B1 (left panels), -phospho H3 (S10) (middle panels) or -Grb-2 (right panels) antibodies. Grb-2 served as a loading control. (b) U-87MG cells were transfected with Vpr or Vpr  $\Delta(37-50)$  expression plasmids or with empty vector, pcDNA<sub>3</sub>. A total of 50  $\mu$ g of cell extract was western blotted with anti-Ku70, -Ku80 or -Grb-2 antibodies. Grb-2 served as loading control. (c) U-87MG cells were transfected with Vpr or Vpr  $\Delta(37-50)$  expression plasmids as well as the empty vector, pcDNA<sub>3</sub>. Corresponding nuclear extracts were utilized to ligate linear pBluscript KS<sup>+</sup>. The DNA bands are visualized on 0.6% agarose gel containing ethidium bromide. The control reaction represents linear plasmid DNA in the absence of nuclear extract. Arrows indicate positions of the linear plasmid (substrate), dimers and subsequent multimers generated as products as a result of NHEJ. (d) Quantitative evaluation of the results from panel a by densitometric analysis with Scion software ( $n=2$ ). Comparisons between Vpr, Vpr  $\Delta(37-50)$  and untransfected U-87MG cells are shown for the linear plasmid, dimers, trimers and tetramers, respectively. Note a significant decrease (\*) in the intensity of dimers and trimers in Vpr-transfected cells in comparison to Vpr  $\Delta(37-50)$ -transfected cells and the empty vector.

Phosphorylated S10 of H3 was detected in mock, adeno-null and adeno-Vpr  $\Delta(37-50)$ -infected cells, which means that these cells progress from G<sub>2</sub> to M phase (middle panels, Mock, ad-null, ad-Vpr  $\Delta(37-50)$  rows). Grb2 was the loading control (right panels).

The data described in Figure 1 showed Vpr causes several types of aberrations including chromosomal rearrangements and fusions. Fusions take place at the ends of the chromosome, which when lacking telomeric repeats are liable for end-to-end fusion and exonucleolytic degradation. Such events could affect the status of telomeric proteins, for example Ku (de Lange, 2002). Ku is a component of the nonhomologous end-joining (NHEJ) DNA repair pathway. Therefore, we sought to determine Ku status in Vpr-transfected cells. Extracts prepared from Vpr- or Vpr  $\Delta(37-50)$ -transfected U-87MG cells were subject to western blot analysis using anti-Ku70 and -Ku80 antibodies. As shown in Figure 4b, Ku70 and Ku80 proteins were induced by Vpr (compare lanes 1 and 3). Transfection of the empty plasmid pcDNA<sub>3</sub> alone or of Vpr  $\Delta(37-50)$  did not affect Ku70 or Ku 80 (compare lane 1 to lanes 2 and 4). Grb2 was used as the loading control.

Next, we evaluated the effect of Vpr on NHEJ DNA. NHEJ is a quick but nonspecific way to ligate DSBs, which may introduce mutations into the repaired DNA. We used a cell-free assay to evaluate NHEJ DNA in Vpr-transfected cells (Trojanek *et al.*, 2003). Figure 4c illustrates the formation of multiple bands from the linear plasmid substrate DNA as a result of NHEJ. A significant reduction in the efficiency of NHEJ was observed in the presence of nuclear extracts from U-87MG-expressing Vpr (lane 3). Densitometry analysis (Figure 4d) was performed for the linear plasmid, dimers and trimers, respectively. The intensity of dimers was reduced more than twofold and the intensity of trimers by sixfold when Vpr-expressing cells were compared to Vpr  $\Delta(37-50)$ -transfected U-87MG cells or to the control cells.

In the next set of experiments, we used an animal model of breast cancer to investigate the cytopathic effects of Vpr on tumor growth. After subcutaneous inoculation and growth of MCA-35 mouse mammary cancer cells, the tumors were treated with Vpr, mutant Vpr  $\Delta(37-50)$  or serum as control. Note that only a single treatment with Vpr protein was administered.

Five days after treatment, the tumors were removed and processed for histological and immunohistochemical analysis. The intratumoral injection of purified recombinant Vpr led to the retardation of the growth of tumors. As shown in Figure 5a (upper panels), the Vpr-treated tumors were significantly smaller than the control tumors (serum and Vpr mutant-injected) by a ratio of 1:3. A full montage of a representative section of the tumors, stained with hematoxylin & eosin (H&E) is displayed in the lower panels. Histologically, the tumors were characterized by numerous sheaths of malignant epithelial cells arranged in islets, and displaying a central area of necrosis, corresponding to a comedo-type cancer. Interestingly, the central areas of necrosis are significantly larger in the smaller, Vpr-treated tumors, as shown by bars in Figure 5b. In the margins of these necrotic areas, the neoplastic cells display nuclear picnosis and fragmentation, which despite the differences in the amount of necrosis, are similar in the treated and control tumors.

Immunohistochemical studies show the absence of Vpr in the control tumors, and the presence of Vpr in the nuclei and cytoplasm of the treated tumor, with a particularly robust expression in the nuclei (Figure 5c, upper panels). Cytochrome *c* was detected in the margin of the necrotic areas in both, the treated and control

tumors; however, its detection appears to be increased in the Vpr-treated tumors (middle panels). Finally, in order to demonstrate the mechanism of cell death, we performed terminal transferase dUTP nick end labeling assays to show the presence of apoptosis. Interestingly, the number of apoptotic cells is remarkably similar, and low between the treated and control tumors (data not shown). However, immunohistochemistry lacking a primary antibody and allowing the nonspecific secondary antibody to penetrate through the damaged membrane of cells undergoing necrosis or necrotic highlighted the significantly larger areas of necrosis in the Vpr-treated tumors (lower panels).

Vpr contains three amphipathic  $\alpha$ -helices connected by loops and folded around a hydrophobic core. Two hydrophobic and hydrophilic domains located on helices I and III of Vpr remain accessible to the solvent. These accessible domains may be involved in protein-protein and/or protein-nucleic acid interactions (Wecker *et al.*, 2002; Morellet *et al.*, 2003).

To the understand Vpr  $\Delta(37-50)$  activities, a model based on the Vpr wt structure has been constructed. The (37-50) domain was removed from the wt Vpr structure (Morellet *et al.*, 2003) and the (1-36) and (51-96) domains were linked together (Figures 6a and c). The NMR distance restraints corresponding to the (1-34)

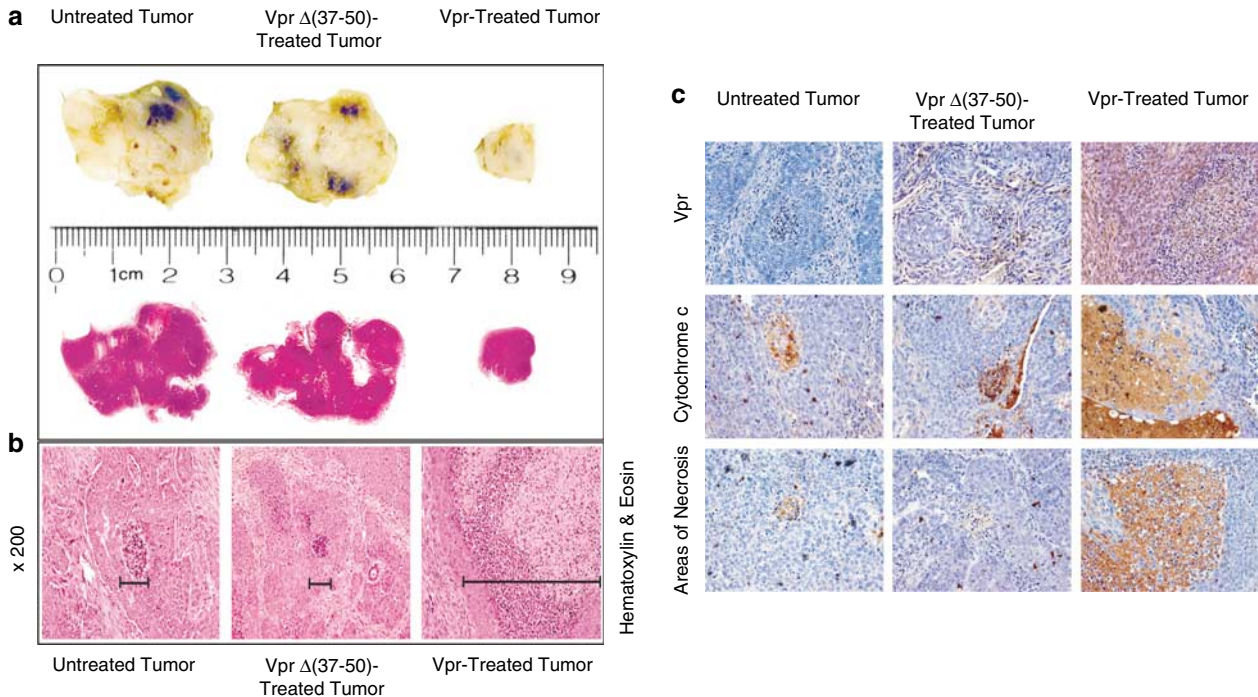


**Figure 5** Effect of wild type and mutant Vpr on tumors in mice. (a) (upper panels) Macroscopic transverse sections of the surgically excised tumors show the size of the tumor mass in Vpr, Vpr-mutant serum treated tumors. The Vpr-treated tumor is significantly smaller by a 1:3 ratio. (lower panels) Full montage of a representative section of treated and control tumors, stained with H&E. (b) H&E sections show a malignant neoplasm with small areas of central necrosis in the control tumors and prominent areas of necrosis in the Vpr-treated tumors. The area of necrosis in each panel is indicated by a bar. (c) (upper panels) Immunohistochemistry for Vpr is negative in the control tumors and positive in the nuclei and cytoplasm of neoplastic cells in the Vpr-treated tumors. (middle panels) Cytochrome *c* was detected in the margins of the necrotic areas in all the tumors, with an increased intensity and number of cells in the Vpr-treated tumor. (lower panels) The significantly larger areas of necrosis in the Vpr-treated tumors are highlighted by a nonspecific immunohistochemical assay.

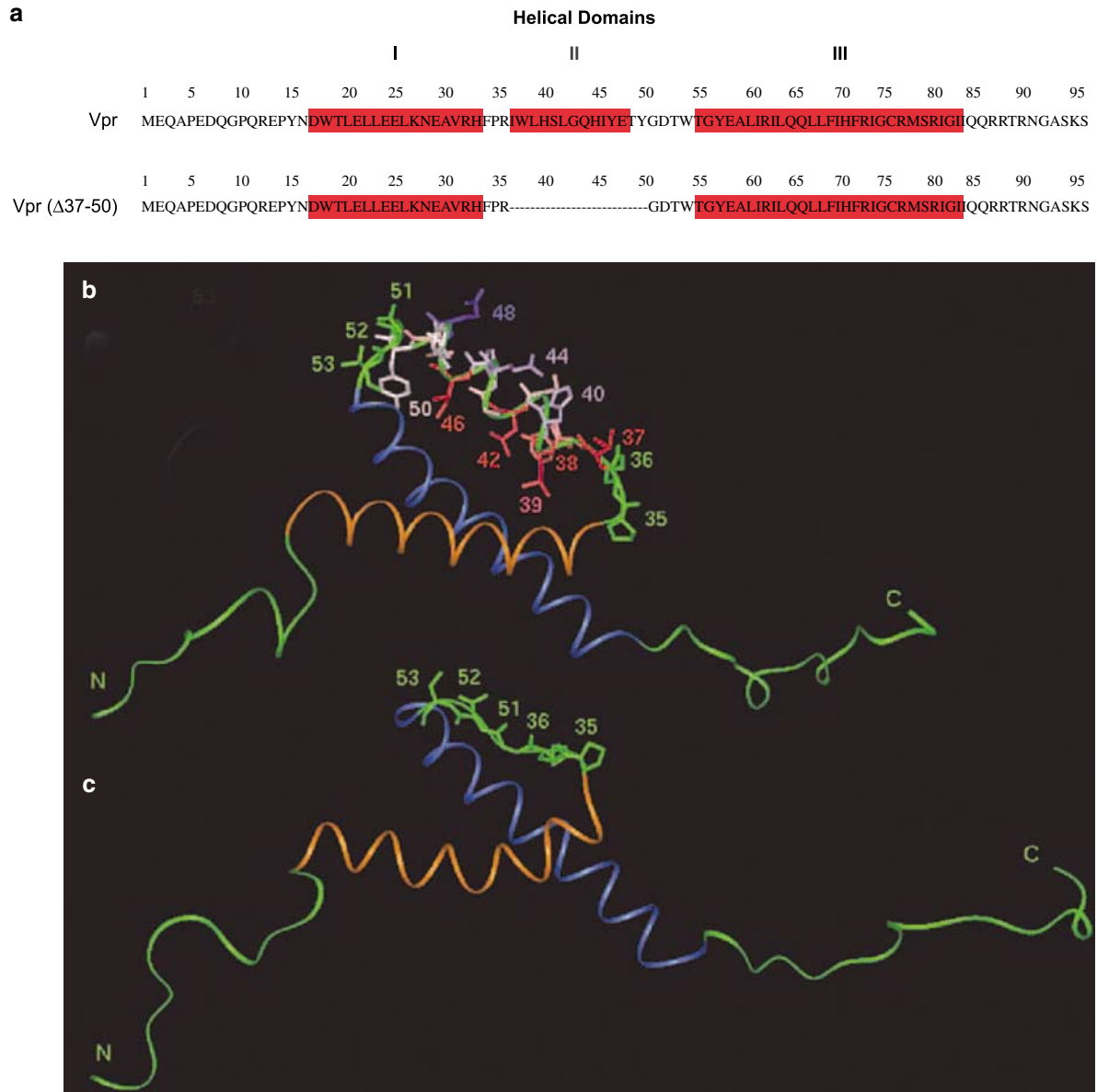


**Figure 6** NMR structure of Vpr. **(a)** Nucleotide sequences of Vpr full length and mutant. The helical domains I, II and III within Vpr are highlighted. **(b)** Vpr structure showing the (37–50) domain. The 35, 36, 51, 52, 53 residues are colored in green. **(c)** Model of the Vpr  $\Delta$ (37–50) structure showing that the interaction between the N- and C-terminal helices of Vpr could still exist, in Vpr  $\Delta$ (37–50).

and (54–96) domains of full-length Vpr were introduced during the molecular structure calculation in order to maintain the (15–34) and (54–78) region in  $\alpha$ -helices as found in the entire protein. The first and the third helices, found in Vpr, are separated by a flexible domain in Vpr  $\Delta$ (37–50), constituted by the residues 35, 36, 51, 52 and 53. These residues are implicated in the two turns found in the Vpr structure (Morellet *et al.*, 2003). The nuclear overhauser effect (NOE) restraints found in full-length Vpr between the first and the third helices (HI and HIII in Vpr  $\Delta$ (37–50)) were therefore added. Interestingly, all these additional restraints between HI and HIII in Vpr  $\Delta$ (37–50) are satisfied, indicating that the two hydrophobic domains of Vpr  $\Delta$ (37–50) can interact with each other without

any hindrance in spite of the short linker between HI and HIII. The two  $\alpha$ -helices could adopt the same orientation in Vpr  $\Delta$ (37–50) than HI and HIII in full-length Vpr (Figures 6b and c). Thus, it appears that the amino acids between positions 37 and 50, such as tryptophan (W38), histidine (H40), glutamine (Q44), glutamic acid (E48) and tyrosine (Y49), hanging at the periphery of the loop might be more involved in interacting with telomeric DNA, telomerase and/or nucleoproteins.

Taken together, these findings lead us to postulate that the sequences spanning aa 37–50 within the wt Vpr may provide opportunities for cancer chemoprevention, treatment of AIDS and a number of other diseases for which effective therapy is not available.

## Discussion

In this study, we identified the Vpr domain(s) involved in DNA damage. We examined several Vpr mutants and demonstrated that the region encompassing amino acids 37–50 within this viral protein is responsible for this function. We found that Vpr  $\Delta(37-50)$  is a stable protein and has the ability to activate HIV-1 gene expression while removal of residues 37–50 from Vpr renders it unable to cause cell cycle arrest. Interestingly, Vpr retains its ability to cause DNA damage in the absence of its C-terminal domain. Note that the C-terminal domain of Vpr has been found to be responsible for cell cycle arrest (Mahalingam *et al.*, 1997a; Zhou *et al.*, 1998). Truncation of, or amino acid substitution in this region results in failure of induction of cell cycle arrest (Mahalingam *et al.*, 1997a; Zhou *et al.*, 1998). Mutation analysis indicated that induction of G<sub>2</sub> arrest depended particularly on the isoleucine residues at positions 74 and 81 in the putative leucine zipper-like domain (Nishizawa *et al.*, 1999). Five of the six Vpr mutations in this region affected G<sub>2</sub> arrest; H71R, H78R and R88K reduced G<sub>2</sub> arrest, while S79A and R90K enhanced G<sub>2</sub> arrest (Chen *et al.*, 1999). We conclude that, in order to cause cell cycle arrest, Vpr requires the presence of helical domains II and III.

In most cells, Ku proteins (70 and 80) are located in the nucleus where they play a role in NHEJ, which is involved in DSB repair (Labhart, 1999; de Lange, 2002). Two DSBs on the same DNA molecule lead to the excision of the internal fragment, which can be deleted, inverted or translocated. Among the different rearrangements, deletions are two- to eightfold more frequent than inversion. This may be due in part to the fact that deletion and inversion require one and two ligation events, respectively (Guirouilh-Barbat *et al.*, 2004). Our results demonstrated that only full-length Vpr affects Ku endogenous levels and disturbs Ku's protective role by preventing NHEJ. This finding correlates with the previously described results in the literature (Majone and Jeang, 2000), where it has been found that HTLV-1 Tax protein interferes with the protective cellular mechanism(s) used normally for stabilizing DNA breaks and affects Ku80 endogenous levels as well NHEJ (Majone and Jeang, 2000; Majone *et al.*, 2005). Thus, we concluded that involvement of viral proteins in DNA damage is not without a precedent.

Besides NHEJ, induction of Ku70 and Ku80 also leads to their translocation and involvement with Bax protein to trigger the apoptotic pathway (Muller *et al.*, 2005). Thus, one can speculate that in addition to DNA damage, Vpr may use Ku family members to trigger the mitochondrial apoptotic pathway. This correlates with observations described previously, where it was reported that HIV-1 uses the pro-apoptotic abilities of Vpr as a strategy to escape immune attack (Gougeon, 2003). However, the exact mechanisms used by Vpr to cause such damage are not fully understood. One possibility is that it is mediated through the physical interaction between Vpr and hHR23A, a protein involved in DNA repair (Gragerov *et al.*, 1998). We previously reported

that association of Vpr with hHR23A promotes the dissociation of hHR23A-S5A complex (Hiyama *et al.*, 1999). Once released, the proteasome subunit, S5A, triggers the DNA damage pathway (BE Sawaya, unpublished data). This observation is in accordance with the study performed by Zhu *et al.* (2001), where they demonstrated that hHR23A inhibits the transcriptional activity of p53 and results in a decreased steady-state protein level of cellular p53. The inhibitory effect of hHR23A was neutralized by the coexpression of Vpr.

The ability of Vpr to affect tumor growth is not without precedent. Studies have demonstrated that Vpr-transfected melanoma cells inoculated into syngenic C57BL/6 mice showed a markedly reduced ability to form tumors *in vivo* (Mahalingam *et al.*, 1997b). These results led the authors to suggest that Vpr has tumor suppressor effects, likely mediated by transcriptional regulation of host cell gene expression. In another study, using AT-84 oral cancer cells to create oral squamous cell carcinomas, a single intratumoral injection of the Vpr lentiviral vector was proven to significantly reduce the primary tumor volume and also regressed tumors in more than 40% of animals (Pang *et al.*, 2001). Further, our results with regard to the inhibition of tumor growth are similar to the data reported by other investigators utilizing subcutaneous B16 melanoma tumor model. McCray *et al.* (2006) used electroporation to introduce plasmid DNA expressing Vpr into tumor cells. In addition to the striking tumor growth inhibition, we also observed necrotic areas in the tumors upon histological analysis. This observation is markedly different from earlier studies reported. We are of the opinion that the differences noted might be related to the experimental setting, such as the use of recombinant Vpr protein, mode of delivery and the use of a different model system. The necrotic region may result from the changes in cells via a combination of endogenous and Vpr-induced cytotoxicity. As Vpr has been shown to enter cells (Henklein *et al.*, 2000; Sherman *et al.*, 2001; Nakamura *et al.*, 2002), it is possible that the necrotic regions may result from spreading of Vpr from the site of inoculation.

Using molecular dynamic simulations, we constructed a model of Vpr  $\Delta(37-50)$ , which could help to understand the biological activity of this mutant when compared to the full-length protein. It has been shown that residues (15–34) and (54–78) within the full-length Vpr adopt an  $\alpha$ -helix structure in the (1–51) Vpr and (52–96) Vpr domains, respectively (Schuler *et al.*, 1999; Wecker and Roques, 1999). We consider it likely that these residues will adopt the same conformation in Vpr  $\Delta(37-50)$ . Therefore, in order to maintain the  $\alpha$ -helix conformations in Vpr  $\Delta(37-50)$ , the NMR restraints corresponding to the (1–34) and (54–96) regions, previously used to determine the full structure of Vpr, were introduced in these calculations (Morellet *et al.*, 2003). In wt Vpr, the hydrophobic domains of the first and third helices, constituted respectively by the Leu20, Leu23, Leu26, Ala30, Val31 and Val57, Leu60, Ile61, Leu64, Leu68, Phe72 residues, interact to each others, in order to maintain the three-dimensional structure of the

protein. The probability that these two hydrophobic domains interact in Vpr  $\Delta(37-50)$  is very high (Figure 6c). In the proposed model (Figure 6c), the acidic residues of Vpr, located in the first helical domain (Asp17, Glu21, Glu24, Glu25, Asn28 and Glu29) remain accessible for interactions with components of the cellular machinery. In fact, the residues Leu20, Leu23, Leu26, Ala30, Val31 and Val57, Leu60, Ile61, Leu64, Leu68, Phe72 residues located respectively on helix I and helix II in Vpr  $\Delta(37-50)$  and in helix I and helix III in Vpr interact to each other to promote the three-dimensional structure of Vpr. These residues are not thus accessible for other interactions. On the contrary, the hydrophobic residues, Trp18, Leu22, Leu26 and Ile63, Leu67, Ile70, Ile74 located on helix I and II respectively remain accessible to the solvent. The hydrophilic accessible domains are constituted by the acidic residues Asp17, Glu21, Glu24, Glu25, Asn28, Glu29 on helix I, and by basic residues Arg62, Arg73, Arg77 and Gln65, Gln66 on helix II and Arg80, Arg87, Arg88, Arg90, Lys95. These residues are still accessible for interaction with other proteins.

The probability that these two hydrophobic domains interact in Vpr  $\Delta(37-50)$  is very high. Therefore, we proposed two possible models for Vpr  $\Delta(37-50)$ . Either the one shown in Figure 6c, where the N- and the C-terminal domains do not interact or where they interact and form a leucine zipper between helices I and II of Vpr  $\Delta(37-50)$ , and in this case the N- and the C-terminal domains, known as acidic and basic domains can interact with each other. Further, the basic residues of the C-terminal domain of Vpr  $\Delta(37-50)$  could interact with the acidic residues of the N-terminal domain, which could explain its inability to cause G<sub>2</sub> arrest. In addition, it has been found that the C-terminal basic region of Vpr was critical for Vpr-DNA or Vpr-RNA interactions (Tachiwana *et al.*, 2006). Therefore, the intermolecular interactions between the basic residues of the C-terminal domain of Vpr  $\Delta(37-50)$  and the DNA may compete with the intermolecular interactions between the basic and acidic residues of the C- and N-terminal domains, respectively. This competition and interaction could be implicated in the DNA damage.

Our cytogenetic data revealed that one of the main targets of the helical domain II of Vpr, and also cisplatin in the treated cultures, is the telomeric region. For instance, the terminal breakage and rejoining, due to the DNA double-strand break at the telomeres, were exhibited in the formation of dicentric, quadriradial and complex configurations of the chromosomes. It is well known that telomeres, which are made of multiple repeats of (TTAGGG)<sub>n</sub>, play a pivotal role in the structural integrity and stability of chromosomes (Baumgartner and Lundblad, 2005). Therefore, any deletion, damage or deterioration of any of telomeres will not only activate the cell cycle arrest check point, but also will induce the genomic instability, structural disintegration of chromosomes and eventually aneuploidy. Aneuploidy is one of the commonly found chromosomal anomalies in most of the solid tumors. Furthermore, metaphases with separated sister

chromatides and diplochromosomes in both Vpr and cisplatin indicate that the molecular insult was not limited to the double-strand DNA break and rejoining at the telomeres, but could also implicate other associated proteins during the cell division. In the light of this molecular mimicry between Vpr and cisplatin, which is exhibited at the chromosomal level, we are contemplating to elucidate the precise interaction of Vpr with nuclear proteins especially telomerase. Since considerable data are available on the DNA alkylation and protein-binding characteristics of cisplatin, it would be very interesting to determine the molecular nature of interaction of Vpr with nuclear proteins in a similar manner.

In summary, we have found that the 37–50 aa sequence of full-length Vpr is involved in DNA damage, disrupted the cell cycle and exhibited a molecular mimicry to cisplatin. In view of these observations, it will be important to further investigate the significance and therapeutic implication of this Vpr domain (37–50), especially for chemoprevention of cancer, AIDS and other pathologies.

## Materials and methods

### *Plasmids, cell culture and transfection assays*

The pcDNA<sub>3</sub>-Vpr full length and its deletion mutants, EGFP-Spectrin, EGFP-Vpr and HIV-LTR-CAT constructs were described previously (Sawaya *et al.*, 1998, 1999, 2000). The human astrocytic cell line, U-87MG, was maintained in Dulbecco's modified Eagle's medium (DMEM) containing 10% fetal calf serum (FCS) and supplemented with antibiotics. Cells were transfected with 0.5  $\mu$ g of reporter plasmid (HIV-LTR-CAT) or co-transfected with 1  $\mu$ g of various expression plasmids as described previously (Amini *et al.*, 2005). The amount of DNA used for each transfection was normalized with pcDNA<sub>3</sub> vector plasmids. Each transfection was repeated multiple times with different plasmid preparations. Cell extracts were prepared 48 h after transfection, and CAT assays were performed as described previously (Sawaya *et al.*, 1998).

### *Cell cycle analysis*

U-87MG cells were transfected with EGFP-spectrin and/or Vpr (wt and mutant) expression plasmids by the calcium phosphate precipitation method (Sawaya *et al.*, 1998). At the indicated times following transfection, the cells were collected. The EGFP-positive and -negative cells were pelleted and resuspended in 70% ice-cold ethanol for 30 min. Following a wash with phosphate-buffered saline (PBS) containing 1% fetal bovine serum, the cells were incubated in PBS containing RNase A (50  $\mu$ g/ml) and propidium iodide (40  $\mu$ g/ml) for 30 min at 37°C. The cellular DNA content was analysed with a FACS scan apparatus. The DNA profile was analysed by the Multicycle AV program (Phoenix Flow System, San Diego, CA, USA).

### *Western blotting*

U-87MG cells were transfected with Vpr (wt and mutant) expression plasmids. Forty-eight hours posttransfection, 50  $\mu$ g of cell extracts were subjected to western blot analysis using anti-Vpr, anti-cyclin B1 or anti-phosphorylated histone H3 (S10) antibodies. Anti-Grb2 antibody was used as a protein-loading control (Claudio *et al.*, 2006).

### Vpr antibody

Vpr peptide from the C-terminal domain of Vpr (HIV-1 NL4-3 Vpr amino acids 81–96, HFRIGCRSHRIGITRQRRARN-GASRS) (purchased from Lampire Biological Lab, Pipersville, PA, USA) coupled to keyhole limpet hemocyanin was used to immunize three rabbits three times. Rabbit anti-Vpr serum recognized recombinant Vpr, Vpr from HIV-1-infected cells and Vpr in the serum of HIV-positive individuals in enzyme-linked immunosorbent assay and western immunoblot and did not react with any other cellular or viral proteins.

### Cytogenetic assays and chromosomal aberrations

U-87MG cells were transfected with 1  $\mu$ g of plasmids encoding full-length Vpr or its deletion mutants for 48 h. Two hours before termination of the experiments, Colcemid (0.1  $\mu$ g/ml) was dispensed in each culture. Metaphases were collected and hypotonized in 75 mM KCl for 5–10 min. After which the cells were fixed in methanol: acetic acid (3:1, v/v) for 5–10 min. The air-drop method was used to spread the chromosomes on a glass slide (Siddiqui *et al.*, 1988). Air-dried slides were subsequently stained with Giemsa (10%) for 10 min, and mounted on Permount. All the slides were observed under a Zeiss light microscope using  $\times 100$  objective lens. However, selected photomicrographs were taken under a Nikon light microscope using  $\times 100$  objective lens. For positive control, cells were treated for 18 h with 1.5  $\mu$ g/ $\mu$ l cisplatin, an alkylating agent known to cross-link with DNA, and consequently induce DNA damage and chromosomal aberrations, and treated as described above.

### Recombinant adenoviruses and infection

Full-length and deletion mutant Vpr were amplified by PCR and cloned into the *Bam*HI/*Hind*III sites of pDC516 under the control of the murine cytomegalovirus promoter. Adeno-Vpr recombinant plasmids containing Vpr sequences (full length and mutant) were transfected into HEK-293 cells with pBHGfrt (del) E1, 3FLP, a plasmid that provides adenovirus type-5 genome deleted in E1 and E3 genes. Plaques of recombinant adenovirus arising as a result of frt/FLP recombination were isolated, grown and purified by cesium chloride density equilibrium banding. Empty shuttle plasmid, pDC515, was used to construct control adenoviral vector (Adeno-null, a virus without any transgene). U-87MG cells were infected with adenoviral vectors at a multiplicity of infection of 5 PFU/cell. After 24 h, the cells were washed and prepared for immunocytochemistry.

### Immunocytochemistry

Cells were plated on poly-L-lysine-coated glass chamber slides and allowed to attach overnight. U-87MG cells were transfected with 1  $\mu$ g of Vpr (wt or mutant) expression plasmid. Cells were then fixed for 3 min in ice-cold acetone, followed by washing with PBS. After blocking with 2% normal rabbit serum for 2 h, slides were incubated in primary antibody (Vpr) overnight at room temperature. Cells were then washed in PBS, incubated in anti-rabbit fluorescein isothiocyanate-conjugated secondary antibody for 2 h at room temperature in the dark, rinsed with PBS and mounted in an aqueous mounting medium (Vector Laboratories, Burlingame, CA, USA) (Claudio *et al.*, 2006).

### Preparation of bacterially expressed Vpr

Plasmid pGEX-2T-Vpr (full length and deletion mutant) fusion proteins were prokaryotically expressed and purified as described previously (Mameli *et al.*, 2007). Briefly, bacteria containing the expression plasmids were grown to an OD<sub>600</sub> of

0.6 and induced with 300  $\mu$ l isopropyl- $\beta$ -D-thiogalactoside (1 M) for 90 min at 37°C. Protein extract was prepared and the fusion protein was purified with glutathione agarose beads and eluted with freshly made 50 mM Tris (pH 7.4) containing 15 mM glutathione. Next, 10  $\mu$ l of thrombin solution (10 cleavage units) was mixed with eluted fusion proteins at 22°C for 16 h. Glutathione S-transferase (GST) was then removed by removing glutathione by extensive dialysis (2000 volumes) against 1  $\times$  PBS followed by column purification on Glutathione Sepharose 4B. The integrity and purity of the GST fusion proteins were analysed by sodium dodecyl sulfate-polyacrylamide gel electrophoresis followed by Coomassie blue staining. Known amounts of bovine serum albumin were included as control on the same gel. For long storage at  $-70^\circ\text{C}$ , glycerol was added to a final concentration of 10%.

### Mice tumors

A total of  $6 \times 10^5$  of mouse mammary carcinoma (MCa-35) cells were injected into the mammary fat pad of C3H/HeJ female mice. After the tumors reached 1.5 cm<sup>3</sup>, Vpr protein was injected into the center of the tumors with a 30-gauge needle at a dose of 1 mg/kg. Controls were untreated tumors and tumors injected with Vpr $\Delta$ (37–50). Five days post-treatment, the tumors were surgically removed and placed into a 10% formalin solution for further processing. Sections of 4  $\mu$ m in thickness were cut and placed in electromagnetically charged slides and H&E staining was performed for routine histological evaluation.

### Histology and immunohistochemistry

After euthanasia, tumors were removed, fixed in formalin and embedded in paraffin. Sections of 4  $\mu$ m in thickness were cut and stained with H&E for routine histological analysis. Immunohistochemistry was performed using the avidin-biotin-peroxidase technique, according to the manufacturer's instructions (Vector Laboratories). After deparaffination and hydration through alcohol and water, sections were placed in citrate buffer (pH 6.0) at 95°C for 30 min for nonenzymatic antigen retrieval and treated with H<sub>2</sub>O<sub>2</sub> in methanol for endogenous peroxidase quenching. Sections were then blocked with normal goat serum and incubated with a rabbit polyclonal anti-Vpr or a mouse monoclonal anti-cytochrome *c* antibody overnight. After rinsing with PBS, sections were incubated with a goat anti-rabbit or anti-mouse biotinylated secondary antibody for 1 h, then with avidin-biotin-peroxidase complexes (ABC Kit, Vector Laboratories) and then sections were developed with diaminobenzidine (Sigma, St Louis, MO, USA), and finally sections were counterstained with hematoxylin and mounted.

### Nonhomologous end joining

The cell-free NHEJ assay was followed (Labhart, 1999), and nuclear lysates were prepared as previously described (Trojanek *et al.*, 2003). Briefly, NHEJ reactions were performed in the following conditions: 50  $\mu$ g of nuclear lysate; 1 mM ATP; 0.25 mM dNTPs; 25 mM Tris-acetate (pH 7.5); 100 mM potassium acetate; 10 mM magnesium acetate; and 1 mM dithiothreitol. After 5 min of preincubation at 37°C, the reaction mixture was supplemented with the substrate (500 ng of *Xho*I-*Xba*I linearized pBluescript KS<sup>+</sup>). The reaction was incubated for 1 h at 37°C to ligate the plasmid and treated with proteinase K to digest DNA-bound proteins. Products of the NHEJ reactions were resolved in 0.6% agarose gel containing 0.5  $\mu$ g/ml of ethidium bromide.

### NMR structure

Calculations were performed with the Discover/NMRchitect software package from Accelrys with the Amber forcefield using a dielectric constant,  $\epsilon = 4r$ , in order to diminish *in vacuo* electrostatic effects. Fifty initial structures for Vpr  $\Delta(37-50)$  were generated using simulated annealing, followed by energy minimization until a maximum gradient value of 0.01 kcal/mol/Å under NMR restraints determined for wt Vpr. The restraints found for the 1–34 and 56–96 domains of Vpr were introduced as the restraints found between helical domains I and III and in Vpr full length and corresponding to helical domain I and II in Vpr  $\Delta(37-50)$ . The 20 structures that had the lowest total energy were used for the final structural analysis. To evaluate the stability of this model, molecular dynamics simulations were done on the structure that had the lowest energy. The NMR distance restraints obtained for Vpr, and corresponding to the remaining residues in Vpr  $\Delta(37-50)$  were used to maintain the two  $\alpha$ -helices close to each others.

### References

Amini S, Mameli G, Del Valle L, Skowronska A, Reiss K, Gelman BB *et al.* (2005). p73 Interacts with human immunodeficiency virus type 1 Tat in astrocytic cells and prevents its acetylation on lysine 28. *Mol Cell Biol* **25**: 8126–8138.

Amini S, Saunders M, Kelley K, Khalili K, Sawaya BE. (2004). Interplay between HIV-1 Vpr and Sp1 modulates p21(WAF1) gene expression in human astrocytes. *J Biol Chem* **279**: 46046–46056.

Ayyavoo V, Mahboubi A, Mahalingam S, Ramalingam R, Kudchodkar S, Williams WV *et al.* (1997). HIV-1 Vpr suppresses immune activation and apoptosis through regulation of nuclear factor kappa B. *Nat Med* **3**: 1117–1123.

Baumgartner BL, Lundblad V. (2005). Telomere identity crisis. *Genes Dev* **19**: 2522–2525.

Chen M, Elder RT, Yu M, O’Gorman MG, Selig L, Benarous R. (1999). Mutational analysis of Vpr-induced G2 arrest, nuclear localization, and cell death in fission yeast. *J Virol* **73**: 3236–3245.

Claudio PP, Cui J, Ghafouri M, Mariano C, White MK, Safak M *et al.* (2006). Cdk9 phosphorylates p53 on serine 392 independently of CKII. *J Cell Physiol* **208**: 602–612.

De Lange T. (2002). Protection of mammalian telomeres. *Oncogene* **21**: 532–540.

Gaynor EM, Chen IS. (2001). Analysis of apoptosis induced by HIV-1 Vpr and examination of the possible role of the hHR23A protein. *Exp Cell Res* **267**: 243–257.

Goh WC, Rogel ME, Kinsey CM, Michael SF, Fultz PN, Nowak MA *et al.* (1998). HIV-1 Vpr increases viral expression by manipulation of the cell cycle: a mechanism for selection of Vpr *in vivo*. *Nat Med* **4**: 65–71.

Gougeon ML. (2003). Apoptosis as an HIV strategy to escape immune attack. *Nat Rev Immunol* **3**: 392–404.

Gragerov A, Kino T, Ilyina-Gragerova G, Chrousos GP, Pavlakis GN. (1998). HHR23A, the human homologue of the yeast repair protein RAD23, interacts specifically with Vpr protein and prevents cell cycle arrest but not the transcriptional effects of Vpr. *Virology* **245**: 323–330.

Guirouilh-Barbat J, Huck S, Bertrand P, Pirzio L, Desmaze C, Sabatier L *et al.* (2004). Impact of the KU80 pathway on NHEJ-induced genome rearrangements in mammalian cells. *Mol Cell* **14**: 611–623.

Hans F, Dimitrov S. (2001). Histone H3 phosphorylation and cell division. *Oncogene* **20**: 3021–3027.

Henklein P, Bruns K, Sherman MP, Tessmer U, Licha K, Kopp J *et al.* (2000). Functional and structural characterization of synthetic HIV-1 Vpr that transduces cells, localizes to the nucleus, and induces G2 cell cycle arrest. *J Biol Chem* **275**: 32016–32026.

Hiyama H, Yokoi M, Masutani C, Sugawara K, Maekawa T, Tanaka K *et al.* (1999). Interaction of hHR23 with S5a. The ubiquitin-like

The long-range restraints introduced during the simulated annealing between helical domains I and II were removed during the molecular dynamics. The NMR restraints found in Vpr for the 35, 36, 51, 52, 53 residues were not introduced in the simulations. The model was minimized using 1000 steps of steepest descent, followed by 1000 steps of conjugate gradient and then subjected to a 250 ps molecular dynamics at 300 K with  $\epsilon = 4r$ . All dynamics were carried out with a time step of 1 fs. The coordinates were saved every 5 ps.

### Acknowledgements

We thank past and present members of the Center for Neurovirology and Department of Neuroscience for sharing reagents. This work was supported by grants awarded by NIH to BES and by Susan G Komen Breast Cancer Foundation Research to MFK.

domain of hHR23 mediates interaction with S5a subunit of 26 S proteasome. *J Biol Chem* **274**: 28019–28025.

Huang MB, Weeks O, Zhao LJ, Saltarelli M, Bond VC. (2000). Effects of extracellular human immunodeficiency virus type 1 vpr protein in primary rat cortical cell cultures. *J Neurovirol* **6**: 202–220.

Jacotot E, Ravagnan L, Loeffler M, Ferri KF, Vieira HL, Zamzami N *et al.* (2000). The HIV-1 viral protein R induces apoptosis via a direct effect on the mitochondrial permeability transition pore. *J Exp Med* **191**: 33–46.

Juan G, Traganos F, James WM, Ray JM, Roberge M, Sauve DM *et al.* (1998). Histone H3 phosphorylation and expression of cyclins A and B1 measured in individual cells during their progression through G2 and mitosis. *Cytometry* **32**: 71–77.

Kino T, Gragerov A, Slobodskaya O, Tsopanichalou M, Chrousos GP, Pavlakis GN. (2002). Human immunodeficiency virus type 1 (HIV-1) accessory protein Vpr induces transcription of the HIV-1 and glucocorticoid-responsive promoters by binding directly to p300/CBP coactivators. *J Virol* **76**: 9724–9734.

Labhart P. (1999). Nonhomologous DNA end joining in cell-free systems. *Eur J Biochem* **265**: 849–861.

Le Rouzic E, Benichou S. (2005). The Vpr protein from HIV-1: distinct roles along the viral life cycle. *Retrovirology* **2**: 11.

Mahalingam S, Ayyavoo V, Patel M, Kieber-Emmons T, Weiner DB. (1997a). Nuclear import, virion incorporation, and cell cycle arrest/differentiation are mediated by distinct functional domains of human immunodeficiency virus type 1 Vpr. *J Virol* **71**: 6339–6347.

Mahalingam S, MacDonald B, Ugen KE, Ayyavoo V, Agadjanyan MG, Williams WV. (1997b). *In vitro* and *in vivo* tumor growth suppression by HIV-1 Vpr. *DNA Cell Biol* **16**: 137–143.

Mahalingam S, Patel M, Collman RG, Srinivasan A. (1995). The carboxy-terminal domain is essential for stability and not for virion incorporation of HIV-1 Vpr into virus particles. *Virology* **214**: 647–652.

Majone F, Jeang KT. (2000). Clastogenic effect of the human T-cell leukemia virus type I Tax oncoprotein correlates with unstabilized DNA breaks. *J Biol Chem* **275**: 32906–32910.

Majone F, Luisetto R, Zamboni D, Iwanaga Y, Jeang KT. (2005). Ku protein as a potential human T-cell leukemia virus type 1 (HTLV-1) tax target in clastogenic chromosomal instability of mammalian cells. *Retrovirology* **2**: 45.

Mameli G, Deshmane SL, Ghafouri M, Cui J, Simbiri K, Khalili K *et al.* (2007). C/EBPbeta regulates human immunodeficiency virus 1 gene expression through its association with cdk9. *J Gen Virol* **88**: 631–640.

McCray AN, Ugen KE, Muthumani K, Kim JJ, Weiner DB, Heller R. (2006). Complete regression of established subcutaneous B16 murine melanoma tumors after delivery of an HIV-1 Vpr-expressing plasmid by *in vivo* electroporation. *Mol Ther* **14**: 647–655.

- Morellet N, Bouaziz S, Petitjean P, Roques BP. (2003). NMR structure of the HIV-1 regulatory protein VPR. *J Mol Biol* **327**: 215–227.
- Muller C, Paupert J, Monferran S, Salles B. (2005). The double life of the Ku protein: facing the DNA breaks and the extracellular environment. *Cell Cycle* **4**: 438–441.
- Nakamura T, Suzuki H, Okamoto T, Kotani S, Atsuji Y, Tanaka T *et al.* (2002). Recombinant Vpr (rVpr) causes augmentation of HIV-1 p24 Ag level in U1 cells through its ability to induce the secretion of TNF. *Virus Res* **90**: 263–268.
- Nishizawa M, Myojin T, Nishino Y, Nakai Y, Kamata M, Aida Y. (1999). A carboxy-terminally truncated form of the Vpr protein of human immunodeficiency virus type 1 retards cell proliferation independently of G(2) arrest of the cell cycle. *Virology* **263**: 313–322.
- Nowak SJ, Corces VG. (2004). Phosphorylation of histone H3: a balancing act between chromosome condensation and transcriptional activation. *Trends Genet* **20**: 214–220.
- Pang S, Kang MK, Kung S, Yu D, Lee A, Poon B *et al.* (2001). Anticancer effect of a lentiviral vector capable of expressing HIV-1 Vpr. *Clin Cancer Res* **7**: 3567–3573.
- Patel CA, Mukhtar M, Pomerantz RJ. (2000). Human immunodeficiency virus type 1 Vpr induces apoptosis in human neuronal cells. *J Virol* **74**: 9717–9726.
- Sawaya BE, Khalili K, Gordon J, Taube R, Amini S. (2000). Cooperative interaction between HIV-1 regulatory proteins Tat and Vpr modulates transcription of the viral genome. *J Biol Chem* **275**: 35209–35214.
- Sawaya BE, Khalili K, Mercer WE, Denisova L, Amini S. (1998). Cooperative actions of HIV-1 Vpr and p53 modulate viral gene transcription. *J Biol Chem* **273**: 20052–20057.
- Sawaya BE, Khalili K, Rappaport J, Serio D, Chen W, Srinivasan A *et al.* (1999). Suppression of HIV-1 transcription and replication by a Vpr mutant. *Gene Therapy* **6**: 947–950.
- Schuler W, Wecker K, de Rocquigny H, Baudat Y, Sire J, Roques BP. (1999). NMR structure of the (52–96) C-terminal domain of the HIV-1 regulatory protein Vpr: molecular insights into its biological functions. *J Mol Biol* **285**: 2105–2117.
- Sherman MP, de Noronha CM, Heusch MI, Greene S, Greene WC. (2001). Nucleocytoplasmic shuttling by human immunodeficiency virus type 1 Vpr. *J Virol* **75**: 1522–1532.
- Sherman MP, Schubert U, Williams SA, de Noronha CM, Kreisberg JF, Henklein P *et al.* (2002). HIV-1 Vpr displays natural protein-transducing properties: implications for viral pathogenesis. *Virology* **302**: 95–105.
- Shimura M, Onozuka Y, Yamaguchi T, Hatake K, Takaku F, Ishizaka Y. (1999a). Micronuclei formation with chromosome breaks and gene amplification caused by Vpr, an accessory gene of human immunodeficiency virus. *Cancer Res* **59**: 2259–2264.
- Shimura M, Tanaka Y, Nakamura S, Minemoto Y, Yamashita K, Hatake K *et al.* (1999b). Micronuclei formation and aneuploidy induced by Vpr, an accessory gene of human immunodeficiency virus type 1. *FASEB J* **13**: 621–637.
- Siddiqui KM, Alexander JA, Struck RF. (1988). Induction of sister-chromatid exchanges in L1210 leukemia cells by new antitumor 2-haloethyl (methylsulfonyl) methanesulfonate compounds. *Mutat Res* **207**: 179–183.
- Stewart SA, Poon B, Song JY, Chen IS. (2000). Human immunodeficiency virus type 1 vpr induces apoptosis through caspase activation. *J Virol* **74**: 3105–3111.
- Tachiwana H, Shimura M, Nakai-Murakami C, Tokunaga K, Takizawa Y, Sata S *et al.* (2006). HIV-1 Vpr induces DNA double-strand breaks. *Cancer Res* **66**: 627–631.
- Trojanek J, Ho T, Del Valle L, Nowicki M, Wang JY, Lassak A *et al.* (2003). Role of the insulin-like growth factor I/insulin receptor substrate 1 axis in Rad51 trafficking and DNA repair by homologous recombination. *Mol Cell Biol* **23**: 7510–7524.
- Wang L, Mukherjee S, Jia F, Narayan O, Zhao LJ. (1995). Interaction of virion protein Vpr of human immunodeficiency virus type 1 with cellular transcription factor Sp1 and trans-activation of viral long terminal repeat. *J Biol Chem* **270**: 25564–25569.
- Wecker K, Morellet N, Bouaziz S, Roques BP. (2002). NMR structure of the HIV-1 regulatory protein Vpr in H<sub>2</sub>O/trifluoroethanol. Comparison with the Vpr N-terminal (1–51) and C-terminal (52–96) domains. *Eur J Biochem* **269**: 3779–3788.
- Wecker K, Roques BP. (1999). NMR structure of the (1–51) N-terminal domain of the HIV-1 regulatory protein Vpr. *Eur J Biochem* **266**: 359–369.
- Zhou Y, Ratner L. (2000). Phosphorylation of human immunodeficiency virus type 1 Vpr regulates cell cycle arrest. *J Virol* **74**: 6520–6527.
- Zhou Y, Lu Y, Ratner L. (1998). Arginine residues in the C-terminus of HIV-1 Vpr are important for nuclear localization and cell cycle arrest. *Virology* **242**: 414–424.
- Zhu Q, Wani G, Wani MA, Wani AA. (2001). Human homologue of yeast Rad23 protein A interacts with p300/cyclic AMP-responsive element binding (CREB)-binding protein to down-regulate transcriptional activity of p53. *Cancer Res* **61**: 64–70.